Formation of Pancakelike Ising Domains and Giant Magnetic Coercivity in Ferrimagnetic LuFe$_2$O$_4$

Weida Wu,[1,*] V. Kiryukhin,[1] H.-J. Noh,[2,+] K.-T. Ko,[2] J.-H. Park,[2] W. Ratcliff II,[3] P. A. Sharma,[4,‡] N. Harrison,[4] Y. J. Choi,[1]
Y. Horibe,[1] S. Lee,[1] S. Park,[1] H. T. Yi,[1] C. L. Zhang,[1] and S.-W. Cheong[1]

[1]*Rutgers Center for Emergent Materials and Department of Physics and Astronomy, Rutgers University,
Piscataway, New Jersey 08854, USA*
[2]*Department of Physics and Electron Spin Science Center, Pohang University of Science and Technology, Pohang, 790-784, Korea*
[3]*NIST Center for Neutron Research, NIST, Gaithersburg, Maryland 20899, USA*
[4]*NHMFL-LANL, Los Alamos, New Mexico 87544, USA*
(Received 23 June 2008; published 24 September 2008)

We have studied quasi-two-dimensional multiferroic LuFe$_2$O$_4$ with strong charge-spin-lattice coupling, in which low-temperature coercivity approaches an extraordinary value of 9 T in single crystals. The enhancement of the coercivity is connected to the collective freezing of nanoscale pancakelike ferrimagnetic domains with large uniaxial magnetic anisotropy ("Ising pancakes"). Our results suggest that collective freezing in low-dimensional magnets with large uniaxial anisotropy provides an effective mechanism to achieve enhanced coercivity. This observation may help identify novel approaches for synthesis of magnets with enhanced properties.

PACS numbers: 75.50.Vv, 75.25.+z, 77.84.−s

Permanent magnets are widely used in modern technology. One of the key characteristics of a magnet is its coercivity, the quantity defining the external magnetic field required to reverse the magnetization direction. Large coercivity is essential for large energy product, a desirable property for many applications [1,2]. Magnetic coercivity is determined by magnetocrystalline anisotropy and the energetics of magnetic domain nucleation and growth [3]. The former is controlled by the spin-orbit coupling, a relativistic effect which is large in heavy elements [4]. Domain wall pinning is also enhanced by large anisotropy. Consistently, the strongest permanent magnets, such as SmCo$_5$ and Nd$_2$Fe$_{14}$B, and best magnetic recording media, such as Fe-Pt [5], usually contain heavy elements. In practice, domain nucleation and growth are the limiting factors in high-coercivity materials. For example, the coercivity of ordinary SmCo$_5$ is as small as 0.1 T, while it increases up to 4 T as nucleation defects are removed through heat treatment [6]. Various approaches to inhibit the domain nucleation and/or growth, and thereby increase coercivity, have been investigated. Examples include introduction of defects impeding domain wall motion by thermal treatment [7], and nanoscale engineering [8] of precisely chosen mixtures of materials with matching magnetic properties.

LuFe$_2$O$_4$ is a magnetic system combining aspects of magnetic frustration and low dimensionality. The hexagonal structure [9] of LuFe$_2$O$_4$ is shown in Fig. 1(a). The structural unit consists of three iron-oxygen bilayers, each consisting of two triangular Fe-O planes, stacked along the c-axis and separated by nonmagnetic Lu ions. The average Fe valence in LuFe$_2$O$_4$ is 2.5. Below $T_{CO} \approx 310$ K, Fe^{2+}/Fe^{3+} charge ordering occurs, and a ferroelectric polarization develops [10,11]. Quasi-two-dimensional

(Q2D) magnetic order takes place at $T_N \approx 220$–230 K, below which the individual Fe-O bilayers order ferrimagnetically, but the interlayer correlations are short-range [12]. The in-plane magnetic order pattern has been obtained by Christianson *et al.* via single crystal neutron scattering refinement without considering charge order [13]. Yet, there are alternative possibilities [14]. Note that for simple antiferromagnetic couplings, both the magnetic interactions within each bilayer and the interlayer interactions are frustrated due to the triangular motif of the crystallographic structure [14]. The system shows strong uniaxial magnetic anisotropy with the easy axis along the c direction. An extraordinary coercivity value of ~10 T at 4.2 K was reported for $H \| c$ in single crystals of LuFe$_2$O$_4$, but the origin of the observed giant coercivity has not been identified thus far [12]. Herein, we report that collective
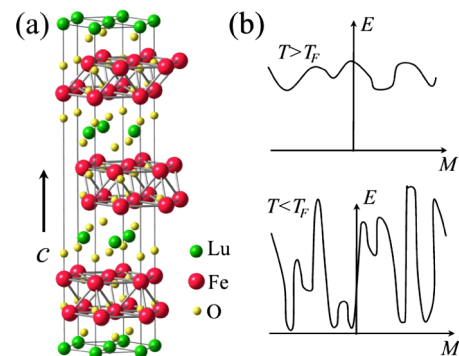

FIG. 1 (color online). (a) The high-temperature unit cell (the full hexagonal prism is shown). Fe-O bilayers are continued beyond the unit cell boundary for clarity. (b) Sketch of the energy landscape above and below the collective freezing temperature T_F [15].

freezing of Ising pancakelike magnetic domains occurs in $LuFe_2O_4$ at low temperatures and show that this magnetic freezing is tightly connected to the enhancement of co-ercivity. This observation opens up new opportunities for searching ultrahigh coercivity materials by utilizing an intrinsic propensity of frustrated magnetic systems towards collective freezing.

Single crystals of $LuFe_2O_4$ were grown using a floating zone technique. Transport and magnetization measure-ments were performed using a Quantum Design PPMS system, except for the magnetization loop at 4 K that was measured using a 60 T pulsed magnet at NHMFL-LANL. Neutron diffraction measurements were carried out on BT-9 triple-axis spectrometer at the NIST Center for Neutron Research. Inline graphite filter, 14.7 meV neutrons, and collimations 40-40-S-40-80 were used. The single crystal data were collected in the (H, H, L) plane using a two-axis mode. The parameters were chosen to achieve integration along the L direction in the reciprocal space. The correla-tion length was obtained from Lorentzian fits of the in-plane scans ($\mathbf{a}^* + \mathbf{b}^*$ direction) convoluted with the ex-perimental resolution. Powder diffraction data were taken using triple-axis mode. The x-ray diffraction data were collected at beam line X22C of the National Synchrotron Light Source. X-ray energy was 10.5 keV. The data were taken for numerous temperatures in the range 10–300 K. Except for overall intensity change, no temperature depen-dence of the scattering pattern was detected. The ab-plane correlation length was obtained from Lorentzian fits of the $\mathbf{a}^*$-axis scans taken at various L positions along the scat-tering rod; the obtained results differ by less than 5 Å. Magnetic force microscopic (MFM) measurements were performed in a homebuilt low-temperature system. The (001) sample surface, prepared by *ex situ* cleaving, was kept in cryogenic vacuum during experiments. MFM im-ages were taken in a frequency-modulated Lift mode, in which the topography and MFM scan lines are interleaved. The lift height was 30 nm.

The magnetic transitions are reflected in the frequency-dependent magnetic susceptibility of single-crystalline $LuFe_2O_4$ shown in Figs. 2(a) and 2(b). The strong anisot-ropy of the system is evident from the $H\|c$ and $H \perp c$ data. Magnetocrystalline anisotropy energy, K, extracted from the corresponding magnetization curves (not shown for brevity) is of the order of 100 K/spin. Besides the peak due to the magnetic transition at T_c, the susceptibility data reveal an additional peak or shoulder at lower temperatures ($T < 150$ K), whose position varies with the frequency, approaching $T_F \approx 80$ K in the static limit. The inset in Fig. 2(b) shows that the frequency dependence of the χ'' feature exhibits the Arrhenius behavior $f = f_0 \exp(-E_a/k_B T)$ with the activation energy $E_a \approx$ 3000 K and $f_0 \approx 4 \times 10^{12}$ Hz. This behavior signals mag-netic freezing [15]. We find that in $LuFe_2O_4$, the parameter $\frac{\Delta T_F}{T_F \Delta \log[f]} \approx 0.1$. This is a typical value for an insulating spin glass, but it is significantly smaller than the values exhib-
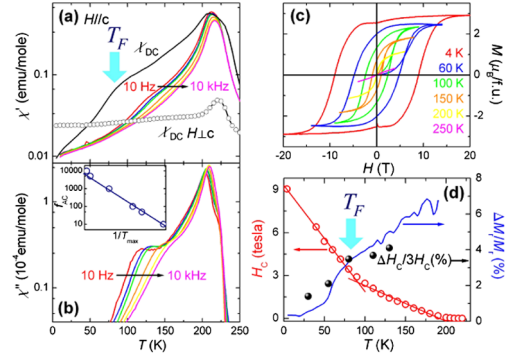

FIG. 2 (color online). (a) Temperature dependence of the static magnetic susceptibility $\chi_{DC} = M/H$ taken on warming (0.2 T, zero field cooled), and the real part of the ac susceptibility χ' at different frequencies (10, 100, 500, 1, 5, and 10 k Hz). The excitation field is 17 Oe. (b) The imaginary part χ'' under the same conditions. The inset shows the frequency-dependent po-sition of the lower-temperature peaklike feature of χ''. (c) $M(H)$ curves at various temperatures. (d) Temperature-dependent mag-netic coercivity (open circles), relative change of the remanent magnetization $|\frac{\Delta M_r}{M_r}|$ with 0.7 K/min and 0.1 K/min warming rates (solid line), and relative coercivity change $|\frac{\Delta H_c}{3H_c}|$ with 0.1 T per minute and 1 T per 3.5 hours sweeping rates (solid circles). The straight lines are guides to eyes. In all panels, the magnetic field is parallel to the c axis, unless specified otherwise.

ited by superparamagnets [15]. This analysis indicates that collective magnetic freezing takes place at T_F.

Below T_c, the system is ferrimagnetic. The $M(H)$ loops ($H\|c$) are shown in Fig. 2(c) for various temperatures, and the obtained coercive fields are shown in Fig. 2(d). Giant magnitude of the magnetic coercivity, approaching 9 T at low temperatures, is observed in our single crystals. Importantly, the coercivity of $LuFe_2O_4$ exhibits a marked increase in the growth rate with the decreasing temperature for $T < T_F$, i.e., in the frozen state. The temperature de-pendence of coercivity is linear for $T < T_F$, which is characteristic to magnetic domains with walls interacting with multiple pinning centers [16]. The increased growth rate of the coercivity may indicate that pinning strength increases dramatically below T_F. This suggests that col-lective magnetic freezing is correlated with the collective domain wall pinning, resulting in the giant coercivity of $LuFe_2O_4$ at low temperature. Investigation of relaxation effects provides further evidence for such connection. The system exhibits extremely slow relaxation (time constants exceeding many days for $T < 150$ K), making detailed time-dependent studies unfeasible. Instead, relaxation ef-fects were characterized using measurements of thermal remanent magnetization $M_r(T)$ taken with two different warming rates (0.7 K/min and 0.1 K/min), and the co-ercivity taken with two different field sweeping rates (0.1 T per minute and 1 T per 3.5 hours). Figure 2(d) shows the relative change of M_r, $|\frac{\Delta M_r}{M_r}|$, in these measurements. Noticeable relaxation (decrease with time) is observed for $T > 100$ K, indicating an unconventional character of

the magnetic state. The relaxation processes are suppressed in the frozen state, as shown by the drop of $|\frac{\Delta M_r}{M_r}|$ in the same temperature region where the anomaly in static susceptibility is observed. Importantly, the relative change of coercivity ($|\frac{\Delta H_C}{H_C}|$) in Fig. 2(d) also exhibits relaxation with a similar temperature-dependent behavior. This freezing behavior coincides with enhancement of coercivity. These data clearly establish an unambiguous link between the relaxation processes controlling the coercivity and the magnetic freezing across T_F. The increased coercivity can be qualitatively explained by reduced sensitivity of the collectively frozen state to external perturbations due to increased free energy barriers between the multiple possible states [15], as illustrated in Fig. 1(b). Below T_F, the barriers are so large that relaxation is suppressed. Therefore, once the system is magnetized, it would remain in this state within experimentally relevant time scales. Flipping the magnetization direction with an applied field has to overcome the increased free energy barriers, resulting in the observed giant coercivity for $T < T_F$. Enhanced coercivity is often observed in the cluster-glass state in amorphous alloys below their freezing temperatures [17], providing further support for the freezing scenario. Note that the coercivity is minute in all these cases probably because of small anisotropy [7]. Freezing of cluster-glass with large anisotropy may result in gigantic value of coercivity.

To gain insight into the nature of the frozen state, we have performed x-ray magnetic circular dichroism (XMCD), neutron scattering, and low temperature MFM measurements. The XMCD results confirmed ferrimagnetic ordering within each Fe-O bilayer with Fe^{2+} (Fe^{3+}) net moment parallel (antiparallel) with the saturation magnetization. We also observed substantial orbital contribution ($\sim 20\%$ of total magnetization) from XMCD experiment, which agrees well with the observed large magnetic anisotropy. The details will be published elsewhere [18].

Neutron diffraction measurements probe the long-range magnetic structure. Previously, it has been reported that a magnetic order with the correlation length of ~ 50 Å is established in each bilayer at low temperatures, and that the interbilayer correlation is very weak [12]. In our sample, the magnetic ordering gives rise to the rods of scattering with the reduced wave vector $(\frac{1}{3}, \frac{1}{3}, L)$. Figure 3(a) shows the temperature dependence of the intensity of the $(\frac{1}{3}, \frac{1}{3}, L)$ magnetic rod integrated in the c direction, and the inverse correlation length within the magnetic bilayers (ξ^{-1}) in a single crystal. Unlike in Ref. [12], quasi-long-range magnetic order ($\xi > 400$ Å) is established in the Fe-O bilayers for $T < 200$ K. Unfavorable sample mosaic prevented us from quantitative studies of the interlayer magnetic correlations using single crystals. However, it was possible to characterize these correlations using powder diffraction data. Figure 3(b) shows scans in the vicinity of the $(\frac{1}{3}, \frac{1}{3}, L)$ magnetic rod for various temperatures. The oscillating pattern after the main peak is caused by the
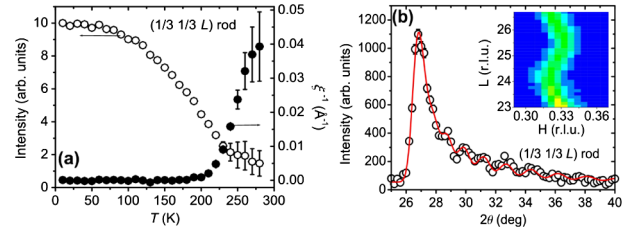

FIG. 3 (color online). (a) Temperature dependence of the integrated intensity of the $(\frac{1}{3}, \frac{1}{3}, L)$ magnetic rod, and the inverse magnetic correlation length in the Fe-O bilayers. The data were taken on single crystal. Error bars are from counting statistics. (b) Powder diffraction scan of the $(\frac{1}{3}, \frac{1}{3}, L)$ magnetic rod at 15 K. The background taken at 300 K is subtracted. The line is a fit to the model described in the text [19]. The inset in (b) shows x-ray scattering pattern in the $(H, 0.33, L)$ scattering plane at 150 K. The scattering results from Fe charge order, and its rodlike shape reflects poor interplanar correlation along the c axis.

correlations between the magnetic bilayers. To analyze these data, we use a model similar to that introduced in Ref. [19]. Each Fe bilayer is described as a long-range-ordered ferrimagnetic plane. The planes are correlated in pairs. The type of the interplane correlation is described by constant C continuously varying from -1 for purely antiferromagnetic correlation to 1 for purely ferromagnetic correlation. The only other parameters of the model are the interplane distance d and the effective mean square displacement in the Debye-Waller factor $\langle u^2 \rangle$. As shown in Fig. 3(b), this model describes the data very well. The low-temperature parameters are $d = 50.6(0.3)$ Å, $C = 0.4(0.1)$, and $\langle u^2 \rangle = 1.6(0.4)$ Å^2; they do not change significantly with temperature below T_c. The stacking pattern of the magnetic planes repeats every 50.6 Å (every six bilayers, i.e., $2c$). The interbilayer correlation is not perfect: for $C = 0.4$, the mean distance between the defects in the stacking pattern is ~ 300 Å, which is comparable to the 156 Å c-axis correlation length of the magnetic ordering observed by Christianson et al. . Unlike our samples, the samples of Ref. [13] ("the ORNL samples") possess long range charge order and do not show any freezing at 80 K. Instead, they exhibit a sharp drop of the $(\frac{1}{3}, \frac{1}{3}, 0)$ peak intensity and of dc magnetization at 175 K. For $T < 175$ K, diffuse magnetic scattering along the c axis is observed in the ORNL samples. Together with the short c-axis correlation, this implies emergence of magnetic disorder [13]. Unfortunately, the data of Ref. [13] are insufficient to establish whether any freezing is associated with the 175 K transition, or if this transition is related to the 80 K freezing in our samples. The nature of the low-temperature phase in the ORNL samples is still an open question [13]. Future ac susceptibility and relaxation measurements of the ORNL samples will be important for understanding the low-temperature phase, and for testing the connection between coercivity and magnetic freezing.

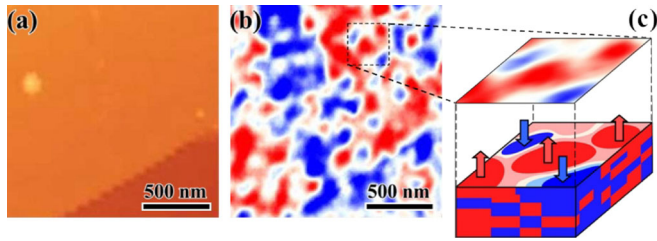Irregular pancakelike magnetic domains (called "Ising pancakes") are observed by MFM for $T < T_c$, as shown in

FIG. 4 (color online).   (a) Topographic image of the cleaved (001) surface at 150 K. The surface contains flat terraces separated by ∼10 nm high steps, one of which is present in the figure. (b) MFM image of the same area at 150 K and 0.5 T (one half of the coercive field at this temperature). The color scale in the topographic (MFM) image is 30 nm (1.5 Hz). (c) A sketch showing the Ising pancake domains in a small area of the MFM image. Arrows indicate magnetization direction.

Fig. 4(b). The in-plane domain size, ∼1000 Å, is larger than the c-axis magnetic correlation length of ∼300 Å measured by neutron scattering. The domain size and pattern do not depend on temperature within experimental error. Magnetic field and temperature dependences of MFM data also show strong memory effect, supporting the aforementioned pinning mechanism for coercivity. Note that the pancakelike domains are very different from the prototypical micron-scale flowerlike pattern characteristic to conventional uniaxial magnets, where the magnetic order is long range [20]. The Ising pancakes can result from a quasi-two-dimensional magnetic order interrupted by defects (quenched disorder), which also serve as pinning centers for domain boundaries between pancakes [21]. We emphasize that the high density of boundaries between Ising pancakes as well as the small size of Ising pancakes is consistent with the presence of freezing transition and the significant pinning of domain boundaries, i.e., the large coercivity at low temperatures. The candidates of quenched disorder in $LuFe_2O_4$ include charge disorder through spin-charge coupling [14], point defects related to ionic off-stoichiometry [22], and structural stacking faults [23]. In our specimens, charge ordering exhibits a temperature-independent in-plane correlation length of 60 Å, as determined by x-ray scattering, see inset in Fig. 3(b). It is completely disordered along the c-axis, which might also indicate the formation of stacking faults [23]. It has been shown that a structural stacking fault could be an effective pinning center for magnetic domain walls [24].

In summary, the c-axis magnetization is determined by the packing configuration of irregular Ising pancakes, which are ∼100 nm in diameter and ∼30 nm thick. We find that collective freezing of these Ising pancakes is remarkably linked to the enhancement of coercivity. While further work is needed to elaborate the microscopic nature of the frozen state in this material, especially in samples with a different degree of disorder [13], our results clearly establish collective freezing as a hallmark of enhanced coercivity. The presence of the large magnetic

anisotropy of the Ising pancakes appears to be crucial for enhanced coercivity, since numerically large coercivity has not been previously observed in cluster-glasses with small anisotropy [17]. Combination of large anisotropy, low dimensionality, and collective pinning or freezing caused by frustration and quenched disorder provides a plausible mechanism to achieve enhanced coercivity. Investigation of similar magnetic systems may help identify novel magnetic compounds with enhanced properties.

*wdwu@physics.rutgers.edu
+Also at: Department of Physics, Chonnam National University, Gwangju 500-757, Korea
‡Current address: Materials Physics Department, Sandia National Laboratories, Livermore, CA 94551
[1] S. Chikazumi, *Physics of Ferromagnetism* (Oxford University Press, New York, 1997).
[2] R. M. Bozorth, *Ferromagnetism* (IEEE Press, Piscataway, 1993).
[3] J. D. Livingston, J. Appl. Phys. **52**, 2544 (1981).
[4] N. Darby and E. Issac, IEEE Trans. Magn. **10**, 259 (1974).
[5] S. Sun *et al.*, Science **287**, 1989 (2000).
[6] M. F. de Campos *et al.*, J. Appl. Phys. **84**, 368 (1998).
[7] P. Tiberto *et al.*, Adv. Eng. Mater. **9**, 468 (2007).
[8] H. Zeng *et al.*, Nature (London) **420**, 395 (2002).
[9] N. Kimizuka, E. Muromachi, and K. Siratori, in *Handbook on the Physics and Chemistry of Rare Earths*, edited by K. A. Gschneider, Jr. and L. Eyring (Elsevier Sci. Press, Amsterdam, 1990), Vol. 13, p. 283.
[10] N. Ikeda *et al.*, Nature (London) **436**, 1136 (2005).
[11] S. W. Cheong and M. Mostovoy, Nature Mater. **6**, 13 (2007).
[12] J. Iida *et al.*, J. Phys. Soc. Jpn. **62**, 1723 (1993).
[13] A. D. Christianson *et al.*, Phys. Rev. Lett. **100**, 107601 (2008).
[14] A. Nagano *et al.*, Phys. Rev. Lett. **99**, 217202 (2007).
[15] J. A. Mydosh, *Spin Glasses* (Taylor & Francis, London, 1993).
[16] P. Gaunt, Philos. Mag. B **48**, 261 (1983).
[17] T. Miyazaki *et al.*, J. Phys. F **18**, 1601 (1988).
[18] H.-J. Noh *et al.* (unpublished).
[19] H. Zhang *et al.*, Phys. Rev. B **45**, 10022 (1992).
[20] A. Hubert and R. Schäfer, *Magnetic Domains* (Springer-Verlag, Berlin, 1998).
[21] K. Ahn (private communication).
[22] S. Funagashi *et al.*, J. Phys. Soc. Jpn. **53**, 2688 (1984).
[23] Y. Zhang *et al.*, Phys. Rev. B **76**, 184105 (2007).
[24] H. Zijlstra and H. B. Haanstra, J. Appl. Phys. **37**, 2853 (1966).